AIP | Applied Physics Letters

Enhanced charge-discharge characteristics of RuO2 supercapacitors on heat-treated TiO2 nanorods

Young Rack Ahn, Chong Rae Park, Seong Mu Jo, and Dong Young Kim

Citation: Appl. Phys. Lett. **90**, 122106 (2007); doi: 10.1063/1.2715038
View online: http://dx.doi.org/10.1063/1.2715038
View Table of Contents: http://apl.aip.org/resource/1/APPLAB/v90/i12
Published by the American Institute of Physics.

Enhanced charge-discharge characteristics of RuO_2 supercapacitors on heat-treated TiO_2 nanorods

Young Rack Ahn[a] and Chong Rae Park
School of Materials Science and Engineering, Seoul National University, Seoul 151-742, Korea

Seong Mu Jo and Dong Young Kim[b]
Optoelectronic Materials Research Center, Korea Institute of Science and Technology, Seoul 136-791, Korea

(Received 22 September 2006; accepted 15 February 2007; published online 20 March 2007)

Electrochemical capacitors based on RuO_2 were prepared onto electrospun TiO_2 nanorods. Further heat treatment of the TiO_2 at 800 °C under nitrogen was found to greatly improve the electrochemical performance of the RuO_2 electrodes, especially at fast charge-discharge rates. The specific capacitance was found to decrease by only 33% when the scan rate increased from 10 to 1000 mV s^{-1} (from 687 to 460 F g^{-1}). The characteristic response time of the RuO_2 electrode was found to be 0.15 s when a heat-treated TiO_2 substrate was used, which is 20 times better than that of the pristine TiO_2 used. © *2007 American Institute of Physics*. [DOI: 10.1063/1.2715038]

Supercapacitors (or electrochemical capacitors) are charge storage devices with a high power density and a long cycle life.[1] Depending on their charge storage mechanism, supercapacitors are classified as either electric double-layer capacitors (EDLCs) or pseudocapacitors. The energy storage mechanism of EDLCs relies on the separation of charges (a non-Faradaic process) at the interface between an electrode and an electrolyte. In pseudocapacitors, by contrast, a Faradaic process occurs in addition to a simple charge separation. Therefore, the charge storage capacity of pseudocapacitors is typically larger than that of EDLCs. For a material to be useful as a pseudocapacitor, it should have several oxidation states, high electrical conductivity, and electrochemical stability. RuO_2 fulfills these requirements, and so is one of the most promising pseudocapacitor materials, but its high cost restricts its bulk commercial use. Thus, the use of thin films[2,3] of RuO_2 and its composites with other materials[4] has been investigated. The use of other transition metal oxides, such as NiO, MnO_2, Fe_3O_4, V_2O_5, etc.,[5–8] has also been investigated, but these materials exhibit inferior specific capacitance or electrical conductivity to RuO_2.

The high power densities and improved frequency responses of supercapacitors are also important properties in electrical vehicle applications.[7,9] We recently reported that the deposit of RuO_2 onto electrospun TiO_2 nanofiber substrates enhances the capacitance of RuO_2 as 687 F g^{-1}.[10] However, these electrodes were found to have low specific capacitance at fast scan rates. The key factors determining the power density and frequency response of an electrochemical capacitor are the resistivities of the electrode material and the electrolyte.[11] Thus, enhancing the electrical conductivity of the TiO_2 substrate is expected to decrease the resistivity of the electrode since the other materials (Ti and RuO_2) have low resistivity.

In this study, the use of potentiodynamically deposited RuO_2 on the heat-treated TiO_2 nanofibers was investigated as electrochemical capacitor applications. The TiO_2 nanofibers were prepared using an electrospinning process; the procedure is described in detail elsewhere.[10,12] Briefly, the precursor solution was composed of titanium (IV) propoxide (Aldrich), acetic acid (Aldrich), and poly(vinyl acetate) (MW=850 000 g mol^{-1}) in *N*,*N*-dimethylformamide. This solution was electrospun onto a titanium plate (99.7%, Aldrich). The as-spun TiO_2 web was then pressed using preheated plates at 120 °C for 10 min. The pressed electrode was then calcined to remove poly(vinyl acetate) and to develop the anatase structure of TiO_2 at 450 °C for 30 min in air. After calcination at 450 °C for 30 min in air, the TiO_2 web was heat treated at 800 °C under a nitrogen atmosphere for 2 h. The electrodeposition of ruthenium dioxide (RuO_2) was then carried out on the heat-treated TiO_2 using a 0.05*M* aqueous ruthenium chloride ($RuCl_3 \cdot nH_2O$, Aldrich) solution. The electrochemical cell used in this study was a three-electrode system, comprising a Pt counter electrode and a

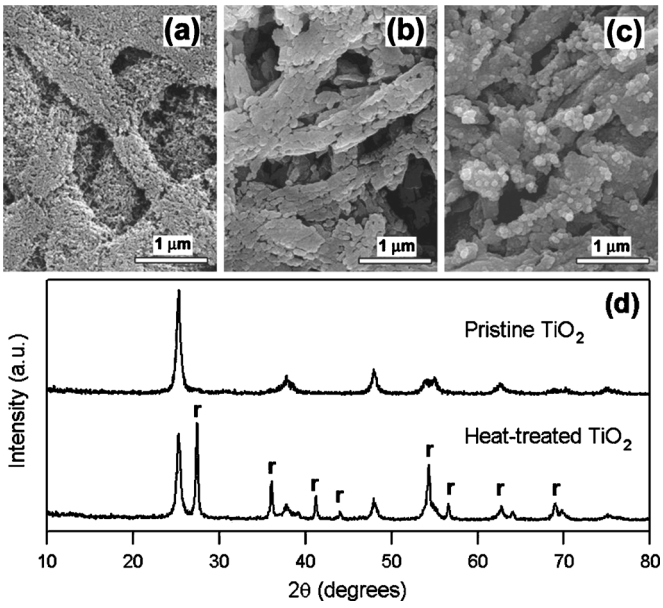

FIG. 1. Scanning electron micrographs of (a) the pristine TiO_2 (A450), (b) the heat-treated TiO_2 (N800), (c) the RuO_2 deposited on the reduced TiO_2, and (d) the x-ray diffraction pattern of pristine (A450) and heat-treated TiO_2 (N800). The rutile peaks are denoted as **r**.

[a]Also with Optoelectronic Materials Research Center, Korea Institute of Science and Technology, Seoul 136-791, Korea.
[b]Author to whom correspondence should be addressed; electronic mail: dykim@kist.re.kr

TABLE I. Preparation conditions and properties of TiO_2 substrates.

Substrate	A450	N800
Temperature (°C)	450	800
Atmosphere	air	N_2
Resistance (Ω)	2.5×10^{10}	3.9×10^{8}
Surface area	138	20

Ag/AgCl reference electrode (with saturated KCl solution). The precursor solution was stirred during the deposition, and the temperature was maintained at 50 °C. RuO_2 was potentiodynamically deposited by cycling the heat-treated TiO_2 electrode between 0.25 and 1.45 V versus the Ag/AgCl reference in $RuCl_3$ solution. The scan rate used for deposition was 300 mV s^{-1}. After deposition, the electrode was heat treated at 175 °C for 1 h. The RuO_2 deposited electrodes were examined using cyclic voltammetry in aqueous 0.5*M* sulfuric acid solution.

After calcination of the hot-pressed electrodes at 450 °C (A450), the original web structure of the as-spun TiO_2 fibers was found to be retained, with each fiber composed, of TiO_2 nanorods, as shown in Fig. 1(a). The Brunauer-Emmet-Teller surface area of the pristine TiO_2 web after calcination was found to be 138 $m^2\,g^{-1}$. After the heat treatment at 800 °C under nitrogen (N800), the surface area of heat-treated TiO_2 decreased to 20 $m^2\,g^{-1}$ due to the crystal growth as well as the coalescence, as shown in Fig. 1(b). The mesopores between nanorods were found to decrease after heat treatment from Barrett-Joyner-Halenda analysis. However, the fibrous structure of TiO_2 was found to be retained also after heat treatment, as shown in Fig. 1(b). Figure 1(c) shows the RuO_2 deposited on the N800 substrate. The macropores between each fiber were found to be retained after RuO_2 deposition. These pores provide a diffusion path for electrolyte into the inner part of the electrode. Figure 1(d) shows the x-ray diffraction patterns of the A450 and N800 substrates. The A450 only produces anatase peaks, whereas rutile peaks of TiO_2 were found in the x-ray diffraction pattern of the N800 after heat treatment at 800 °C under dry nitrogen. The color of the A450, calcined at 450 °C in air, was white, but the N800 was gray. The energy dispersive spectra analysis revealed that the atomic ratio of N800 was Ti(1) vs O(1.91), while the pristine one was Ti(1) vs O(2.01). Thus, the oxygen in the titanium dioxide is only partially removed (~5%), and the oxide is not reduced completely to the metallic state. However, partial deoxidation at an early stage of reduction results in the formation of an electrically conductive oxide phase. The apparent resistance of TiO_2 nanorods was measured using Pt-grid-patterned Al_2O_3 substrates with a 200 μm gap. As presented in Table I, the resistance decreased from 2.5×10^{10} Ω (A450) to 3.9×10^{8} Ω (N800) after heat treatment, which corresponds to 64 times improvement in conductivity.

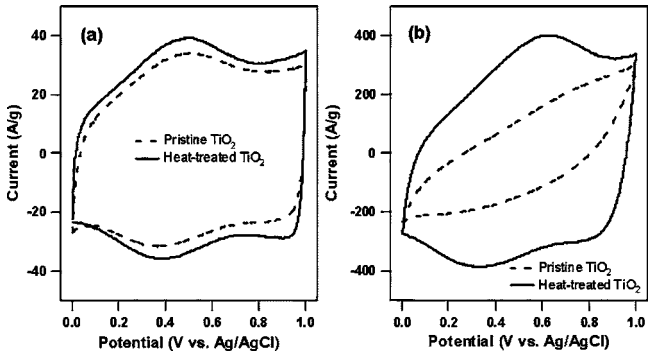

FIG. 2. Cyclic voltammograms of the RuO_2 electrodes based on pristine (A450) and heat-treated TiO_2 (N800) substrates in 0.5*M* H_2SO_4 electrolyte at a scan rate of (a) 50 mV s^{-1} and (b) 500 mV s^{-1}.

Cyclic voltammetry is the appropriate technique for examining a capacitive behavior. It is desirable that the electrochemical capacitor exhibit a rectangular shape and symmetry in the anodic and cathodic sweeps, and a current density of large magnitude in the cyclic voltammogram (CV). Figure 2 shows the CVs of the RuO_2 electrodes. At slow scan rates, the cyclic voltammograms (CVs) of the two different electrodes have a similar shape and current density, as shown in Fig. 2(a). At fast scan rates, however, the shapes of the CVs are quite different. The RuO_2 deposited on the N800 electrode (N800Ru) was found to exhibit a rectangular CV outline even at scan rates faster than 500 mV s^{-1}, whereas the RuO_2 deposited on the A450 electrode (A450Ru) was found to produce a linear shape at that scan rate. Thus, the average current density of the N800Ru electrode was found to be larger than that of the A450Ru electrode. This leads to a substantial difference in the specific capacitances of the electrodes at fast scan rates, as shown in Fig. 3(a). The average specific capacitance was calculated according to

$$C_{sp} = \frac{i}{vw}, \tag{1}$$

where i, v, and w are the average current (mA), the scan rate (mV s^{-1}), and the weight of deposited RuO_2 (g), respec-

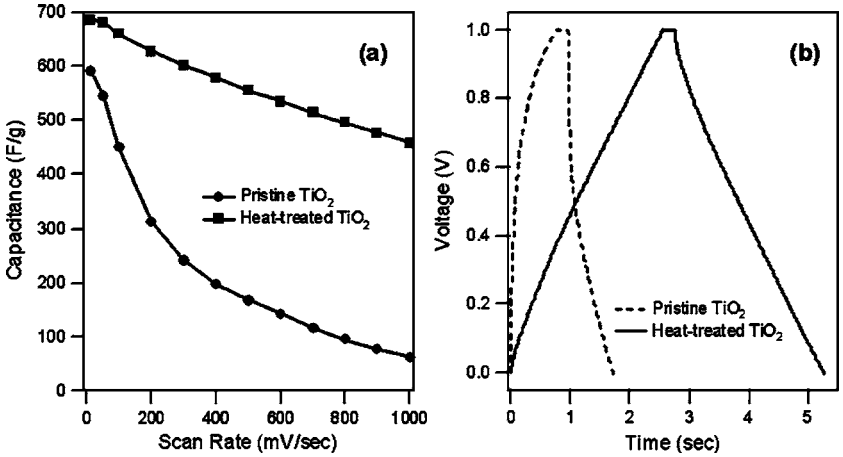

FIG. 3. (a) Variation of specific capacitance calculated from cyclic voltammograms and (b) galvanostatic charge-discharge voltage profiles of pristine (A450Ru) and heat-treated TiO_2 (N800Ru) electrodes at 15 mA cm^{-2}.

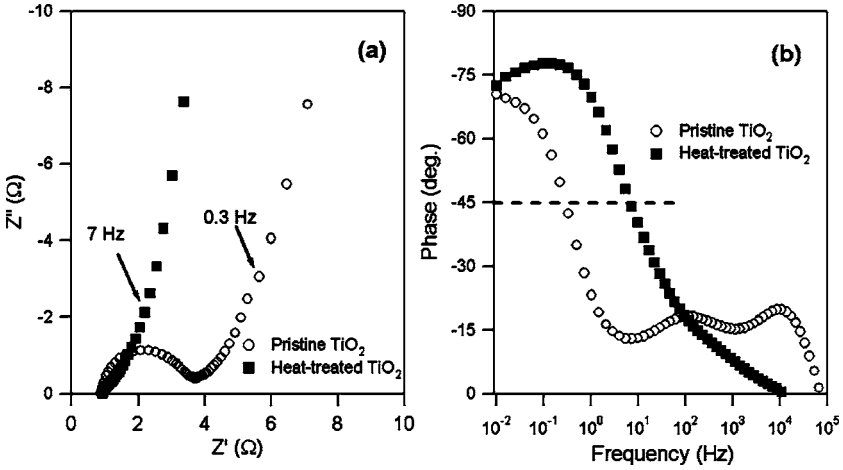

FIG. 4. EIS results conducted on RuO_2 electrodes based on pristine (A450) and heat-treated TiO_2 (N800) in 0.5*M* H_2SO_4 solution. (a) Nyquist and (b) Bode plots.

tively. The variation of specific capacitance of A450Ru and N800Ru electrodes is shown in Fig. 3(a). The specific capacitance of the A450Ru electrode was found to decrease from 593 F g^{-1} at a scan rate of 10 mV s^{-1} to 62 F g^{-1} at 1000 mV s^{-1} (an 89% decrease). However, the specific capacitance of the N800Ru electrode is decreased by only 33% by the use of fast scan rates (from 687 F g^{-1} at 10 mV s^{-1} to 460 F g^{-1} at 1000 mV s^{-1}). Similar results were obtained in galvanostatic charge-discharge tests, in which symmetric full cells (2×2 cm^2) containing these two electrodes and a rayon separator were used. The separator was immersed in 0.5*M* H_2SO_4 before each symmetric cell was assembled. Figure 3(b) shows the galvanostatic charge-discharge voltage profiles for the RuO_2 electrodes at 15 mA cm^{-2}. The specific capacitances at this current density of the A450Ru and N800Ru electrodes were found to be 454 and 164 F g^{-1}, respectively. The decrease in the *iR* drop of N800Ru at this current density compared to A450Ru indicates that the N800 has higher electrical conductivity.

Electrochemical impedance spectroscopy (EIS) was also used to characterize the charge-discharge properties of the pseudocapacitors. The EIS analysis was conducted using an IM6e (Zahner-elektrik) over a frequency range of 10 mHz to 1 MHz at an ac amplitude of 10 mV. Figure 4(a) shows the Nyquist plots for the RuO_2 electrodes. Both the A450Ru and N800Ru electrodes were found to exhibit an almost purely capacitive behavior at low frequencies, as indicated by the vertical lines in these Nyquist plots.[13,14] These electrodes were found to exhibit different behaviors in the high frequency region. The semicircle at high frequencies is found to disappear by using N800Ru electrode. The semicircle at high frequencies is associated with the porous structure of electrode, namely, the semicircle disappeared due to the decrease of mesopores after heat treatment of TiO_2 nanorods. Figure 4(b) shows the Bode plots for the TiO_2-based electrodes. The characteristic response frequency $f_c(\theta=45°)$, which is the frequency at the phase angle (θ) is 45°, is used to characterize the transition from capacitive to resistive behavior.[11,15] The characteristic response time τ_c is also defined as the inverse of $f_c(\theta=45°)$ and characterizes the charge-discharge rate of the system. τ_c was found to be 3.33 and 0.15 s for the A450Ru and N800Ru electrodes, respectively. Thus, the response time was found to improve by a factor of 20 with the use of the N800Ru.

In summary, we have shown that the heat treatment of the TiO_2 substrate enhances the electrical conductivity, hence substantially improving the response time of the RuO_2 electrode. The heat treatment of the TiO_2 substrate not only increases the maximum specific capacitance but greatly enhances the performance at fast charge-discharge rates. The RuO_2 electrode deposited on heat-treated TiO_2 maintains a high capacitance, with only a 33% decrease at a fast scan rate of 1000 mV s^{-1} with respect to the value at 10 mV s^{-1}. Further, the use of the heat-treated TiO_2 enhances the capacitance and the charge-discharge rate by a factor of more than 20 over that of the pristine TiO_2. These results demonstrate the remarkable supercapacitor performance of RuO_2 electrodes deposited on the heat-treated TiO_2 at very fast scan rates and high current densities.

[1] B. E. Conway, *Electrochemical Supercapacitors, Scientific Fundamentals and Technological Applications* (Kluwer, New York/Plenum, New York, 1999).
[2] J. M. Miller and B. Dunn, Langmuir **15**, 799 (1999).
[3] C. Hu and Y. Huang, J. Electrochem. Soc. **146**, 2465 (1999).
[4] Y. G. Wang and X. G. Zhang, Electrochim. Acta **49**, 1957 (2004).
[5] J. K. Chang and W. T. Tsai, J. Electrochem. Soc. **150**, A1333 (2003).
[6] M. Wu, Appl. Phys. Lett. **87**, 153102 (2005).
[7] K. R. Prasad and N. Miura, Appl. Phys. Lett. **85**, 4199 (2004).
[8] T. Cottineau, M. Toupin, T. Delahaye, T. Brousse, and D. Belanger, Appl. Phys. A: Mater. Sci. Process. **A82**, 599 (2006).
[9] K. Chang and C. Hu, Appl. Phys. Lett. **88**, 193102 (2006).
[10] Y. R. Ahn, M. Y. Song, S. M. Jo, C. R. Park, and D. Y. Kim, Nanotechnology **17**, 2865 (2006).
[11] W. Sugimoto, H. Iwata, K. Yokoshima, Y. Murakami, and Y. Takasu, J. Phys. Chem. B **109**, 7330 (2005).
[12] M. Y. Song, Y. R. Ahn, S. M. Jo, D. Y. Kim, and J. P. Ahn, Appl. Phys. Lett. **87**, 113113 (2005).
[13] H. J. In, S. Kumar, Y. Shao-Horn, and G. Barbastathis, Appl. Phys. Lett. **88**, 083104 (2006).
[14] E. Frackowiak and F. Beguin, Carbon **39**, 937 (2001).
[15] P. L. Taberna, P. Simon, and J. F. Fauvarque, J. Electrochem. Soc. **150**, A292 (2003).